New dataset of atmospheric parameters retrieved by PFS-MEx

M. Giuranna[1], P. Wolkenberg[1,2], D. Grassi[1], A. Aronica[1], S. Aoki[3,4,5], D. Scaccabarozzi[6], B. Saggin[6], V. Formisano[1,†], and the PFS team

[1]*National Institute of Astrophysics INAF-IAPS Italy,* [2]*Space Research Centre of Polish Academy of Sciences, Poland,* [3]*Belgian Institute for Space Aeronomy, Belgium,* [4]*Fonds National de la Recherche Scientifique, Belgium,* [5]*Tohoku University, Japan,* [6]*Department of Mechanics, Politecnico di Milano,Italy*

Introduction: We used thermal-infrared spectra returned by the Mars Express Planetary Fourier Spectrometer (PFS-MEx) to derive atmospheric temperature profiles, surface temperatures, and column-integrated optical depths of dust and water ice. More than 3,000,000 spectra have been used to build this new dataset, covering the full range of season, latitude, longitude, and local time. The data presented here span more than seven Martian years (from MY26, Ls = 331°, 10 January 2004 to MY 34, Ls = 21°, 18 June 2017). By exploiting PFS/MEx capability to perform observations at different local times (LT), this dataset allows investigation of the daily cycles of suspended dust and ice. We present an overview of the seasonal and latitudinal dependence of atmospheric quantities during the relevant period, as well as an assessment of the interannual variability in the current Martian climate. Daily variations of Martian aerosols are also presented, including dust during the global dust storm of MY 28, and water ice in the aphelion cloud belt. Atmospheric temperatures and aerosols opacity are successfully retrieved in the polar regions, including the polar nights. Effects of suspended dust on atmospheric temperatures is also investigated. The above atmospheric parameters are also used as input parameters for the self-consistent retrieval of water vapour and carbon monoxide climatology.

PFS Retrievals: The atmospheric parameters presented here are retrieved by means of the algorithm for the scientific analysis of individual calibrated PFS measurements originally developed by **[1]** and recently improved by **[2]**. The improved algorithm uses the optimal estimation method with the Bayesian approach **[3]**, and has also been optimized for the retrieval of dust opacity during strong dust storms. In **Figure 1** we present the dataset of retrieved parameters for more than seven full MYs. A global dust storm occurred in MY 28. The strongest regional dust storm is observed in MY 29. In addition to the aphelion cloud belt (Ls~50°-150°; **[4]**), water ice activity is observed every year during the southern Summer (Ls 270-360°), and especially around Ls=300°, over most southern latitudes and around the equator.
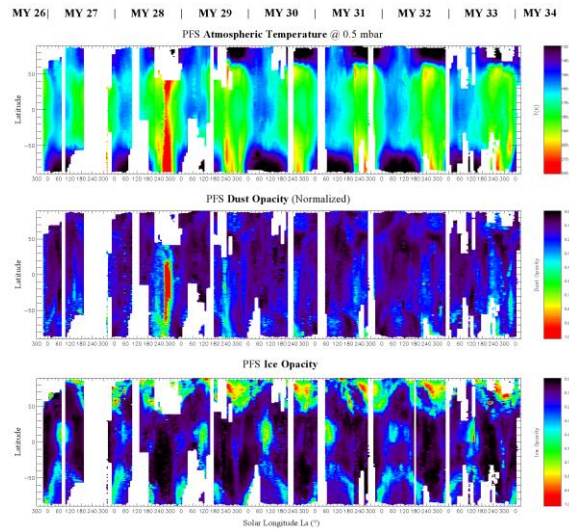

Figure 1: Zonal-mean temperatures at 0.5 mbar (top), dust opacity (middle), and ice opacity (bottom) as a function latitude and Ls and for different Martian Years

Climatology of dust and ice: PFS-Mex observations successfully allows the retrieval of dust and ice opacity over cold-surface areas, night-side regions, and in the polar regions, including the polar nights, where some of the most striking features are observed. Type A, B, and C dust activity, as defined in **[5]**, are consistently observed by PFS and repeats every Martian year. A region of extremely dust clear air generally separates the dust in the winter tropics from aerosol in the winter high latitudes. This feature repeats every year in both hemispheres and has also been observed by MCS **[6]**. It cannot be reproduced by GCM models and a full explanation is still missing.

The PFS ice opacity in the polar regions reveals spatial and seasonal features never observed before, which repeat every year. They are not reproduced by current GCMs, including recent implementations with improved microphysics and radiatively active ice clouds **[7]**.

Climate, circulation and interannual variability: The spatial and temporal coverage of this dataset allows detailed analysis of the Martian climate and circulation. With seven MYs currently covered by PFS observations, investigation of interannual variability of mean

atmospheric parameters is also possible. The zonal-mean temperatures repeats very similarly on Mars each years, although interannual variations ranging from several up to tens of degrees can be observed. Such variations are often, although not exclusively, related to the overall dust content in the Martian atmosphere in the different years.

Effects of dust on atmospheric temperatures: In **Figure 2** we compare temperatures registered during the global dust storm event of MY28 with the temperatures observed for a typical Martian year (MY 30), when regional dust storms occur in the same range of Ls (240-300°). The atmosphere is strongly heated up by absorption of solar radiation due to dust, as expected. During the planet-encircling dust storm of MY28, a net heating is observed for altitudes above the thickest dust layers, where the atmosphere is up to 28 K warmer than for a typical Martian year. However, the infrared radiative cooling rates due to dust cannot be overlooked in the lower altitudes within dusty atmosphere. Especially, at a dust storm event, cooling in the infrared regions is comparable to heating due to absorption of the incident solar radiation by dust, and the thermal structure of the Martian atmosphere is determined by the balance between heating and cooling caused by radiative effects of dust. Solar shielding by thick dust layers may also contribute to the cooling of the lower atmospheric layers. The region of maximum cooling corresponds to the region where maximum dust opacity is observed (0-30° S latitude). PFS result also indicates that, even at out-of-storm events, cooling rate due to dust seems to have the same order as the magnitude of infrared radiative cooling due to CO_2 **[2, 8]**.
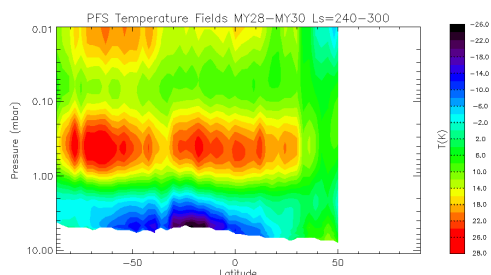

Figure 2: Effect of MY28 dust storm on atmospheric temperatures. MY 28 – MY 30.

Daily cycles of dust and ice: Contrary to TES and MCS data, the PFS dataset presented here allow us to investigate the daily variation of both ice and dust. Exploiting the non-Sun-synchronous nature of Mars Express orbit, PFS performed observations of Martian atmosphere at all local times .

Dust. The mean values of dust opacity during non-dusty seasons and during the global dust storm observed in 2007 will be presented as a function of local time for both hemispheres.

Ice. The aphelion cloud belt is composed of optically thin clouds that form above 10-15 km at low latitudes during northern spring and summer **[4]**. The spatial distribution of nighttime and daytime ice clouds in the aphelion cloud belt as observed by PFS will be shown. Numerical modeling suggests that the tides are strongly influenced by topography **[9]** (primarily by Tharsis and Olympus mons) and thus water ice clouds are mainly found near the topographic features. The variation with local time of the ice opacity observed by PFS in the aphelion cloud belt will also be presented.

Water vapour and carbon monoxide climatology: an algorithm to retrieve water vapour and carbon monoxide is developed and applied to the whole PFS dataset. The computation of synthetic spectra to be compared (best-fit) to the PFS observations relies on the DISORT **[10]** solver implemented in the ARS code **[11]** specifically developed for the analysis of PFS spectra with a full treatment of the Multiple Scattering problem. Typical quality of PFS spectra modelling for H_2O and CO retrievals is shown in **Figure 3**. The retrieval is ongoing. Preliminary results will be presented.
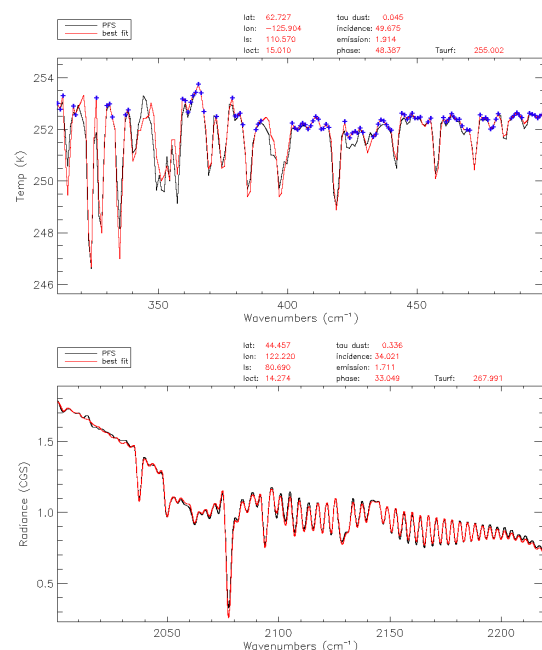

Figure 3: Typical quality of PFS spectra modeling for water vapor (top) and carbon monoxide (bottom) retrievals.

Conclusions: With unprecedented spatial and temporal coverage and details revealed, this dataset offers new challenges to the GCMs and, at the same time, a new reference for the MYs complementary to those observed by TES.

References:

[1] D. Grassi, et al. (2005). Planet. Space Sci., 53, doi:10.1016/j.pss.2005.01.006.

[2] P. Wolkenberg, et al. (2017), Icarus, doi.org/10.1016/j.icarus.2017.10.045.

[3] C.D. Rodgers (2000). Inverse Methods for Atmospheric Sounding: Theory and Practice, World Scientific, Singapore.

[4] R.T. Clancy, et al. (1996), Icarus, 122, doi:10.1006/icar.1996.0108.

[5] D.M. Kass, et al., Geophys. Res. Lett., 43, doi:10.1002/2016GL068978.

[6] N.G Heavens, et al. (2011). J. Geophys. Res., 116, doi:10.1029/2010JE003713.

[7] T. Navarro, et al (2014). J. Geophys. Res., 116, doi:10.1029/2010JE003713.

[8] P. Wolkenberg, et al., this workshop.

[9] D.P. Hinson, et al. (2004). J. Geophys. Res., doi:10.1029/2003JE002129.

[10] K. Stamnes, et al. (1988), Appl. Opt. 27 (12), pp. 2502–2509.

[11] N.I. Ignatiev, N.I., et al. (2005) Planet. Space Sci. 53, 1035–1042.

[12] E. Millour E, et al. (2015) The Mars Climate Database (MCD version 5.2). European Planetary Science Congress 2015, held 27 September – 2 October, 2015 in Nantes, France. EPSC2015-438